EPJ Plus

EPJ.org
your physics journal

Eur. Phys. J. Plus (2014) **129**: 25 DOI 10.1140/epjp/i2014-14025-3

Numerical study of thermally stratified nanofluid flow in a saturated non-Darcy porous medium

Ch. RamReddy, P.V.S.N. Murthy, A.M. Rashad and A.J. Chamkha

Società Italiana di Fisica

Springer

Eur. Phys. J. Plus (2014) **129**: 25
DOI 10.1140/epjp/i2014-14025-3

THE EUROPEAN PHYSICAL JOURNAL PLUS

Regular Article

Numerical study of thermally stratified nanofluid flow in a saturated non-Darcy porous medium

Ch. RamReddy[1,a], P.V.S.N. Murthy[2], A.M. Rashad[3], and A.J. Chamkha[4]

[1] Department of Mathematics, National Institute of Technology Warangal-506004, India
[2] Department of Mathematics, Indian Institute of Technology, Kharagpur-721 302, India
[3] Department of Mathematics, Aswan University, Faculty of Science, 81528, Egypt
[4] Manufacturing Engineering Department, Public Authority for Applied Education and Training, Shuweikh, 70654 Kuwait

Received: 10 July 2013 / Revised: 21 November 2013

Published online: 6 February 2014 –

Abstract. In this paper, we analyze the natural convection flow along a vertical plate in a non-Darcy porous medium saturated with a thermally stratified, electrically conducting nanofluid. The non-linear governing equations and their associated boundary conditions are initially cast into dimensionless forms by local similarity variables. The resulting system of equations is then solved numerically using an implicit finite-difference method. Comparison of the numerical results is made with previously published works for special cases, and shows a good agreement. In order to explore the importance of the various physical parameters involved in this study, a parametric study of the physical parameters is conducted and a representative set of numerical results is presented through graphs.

1 Introduction

In recent years, the conventional heat transfer fluids, for instance, oil, water, and ethylene glycol mixtures, are considered to be poor heat transfer fluids because of their poor thermal conductivity. The application of these fluids as a cooling tool enhances manufacturing and operating costs. Many attempts have been made by several researchers in order to enhance the thermal conductivity of these fluids by suspending nano/micro particles in liquids. But there is no single fluid model which clearly enhances the thermal conductivity of the fluid. Therefore, during the last few years several fluid models were proposed to enhance thermal conductivity of the fluid. One such fluid is the nanofluid (initially introduced by Choi [1]). We may regard a nanofluid as a special sort of multi-component fluid containing nanometer-sized particles (diameter less than 100 nm) or fibers suspended in an ordinary fluid. Undoubtedly, the nanofluids are advantageous, in the sense that they are more stable and have acceptable viscosity and better wetting, spreading and dispersion properties on a solid surface. Nanofluids are used in different engineering applications such as microelectronics, microfluidics, transportation, biomedical, solid-state lighting and manufacturing. The research on heat transfer in nanofluids has been receiving increased attention worldwide. By considering two distinct approaches (*i.e.*, one is that employed by Das *et al.* [2] and another alternative is given by Buongiorno [3]), many researchers have found unexpected thermal properties of nanofluids, and have proposed new mechanisms behind the enhanced thermal properties of nanofluids. Further, a very good collection of published papers on nanofluids can be found in the review papers by Kakac and Pramuanjaroenkij [4].

Due to the practical engineering and industrial applications, the prediction of the heat transfer characteristics of the natural convection of fluids saturating a non-Darcy porous medium, has gained great importance. Nield and Bejan [5] have given a detailed review of the convective heat transfer in Darcian and non-Darcian porous media. Nield and Kuznetsov [6,7] discussed the natural convective boundary layer flows in a porous medium saturated with nanofluids by taking the Brownian motion and thermophoresis effects into consideration. Also, they made the assumption that the nano-sized particles are suspended in uniform distribution in a base fluid to form a nanofluid. When these nanofluids

[a] e-mail: chittetiram@gmail.com

pass through porous media, the suspension of the nanoparticles is maintained by using a surfactant or some surface charge technology to prevent their agglomeration and to avoid being captured by the porous matrix. Several authors, Chamkha *et al.* [8], Khan and Aziz [9] and Gorla and Chamkha [10], to mention but a few, have studied the natural convective transport over different surface geometries in a nanofluid-saturated non-Darcy porous medium.

Many problems on magnetohydrodynamic (MHD) flows of porous media (Darcian and non-Darcian), saturated with Newtonian as well as non-Newtonian fluids, have been analyzed and reported in the literature due to their important technological and industrial applications. Chamkha and Aly [11] obtained a numerical solution of the steady natural convection boundary layer flow of a nanofluid consisting of a pure fluid with nanoparticles along a permeable vertical plate in the presence of magnetic field, heat generation or absorption, and suction or injection effects. Hamada *et al.* [12] reported the similarity reductions for problems of magnetic field effects on the free convection flow of a nanofluid past a semi-infinite vertical flat plate. The steady two-dimensional MHD laminar-free convective boundary layer flows of an electrically conducting Newtonian nanofluid over a solid stationary vertical plate in a quiescent fluid, taking into account the Newtonian heating boundary condition, has been investigated numerically by Uddin [13]. Recently, Kameswaran *et al.* [14] investigated the convective heat and mass transfer in a nanofluid flow over a stretching sheet subject to hydromagnetic, viscous dissipation, chemical reaction and Soret effects.

In many industrial and engineering problems of practical interest, convection flows arise in a thermally stratified environment. The linear case of thermal stratification leads to the stable thermal stratification. For example, the input of thermal energy in enclosed fluid regions, due to the discharge of hot fluid or heat removal from heated bodies, often leads to the generation of a stable thermal stratification. In particular, the study of the heat transfer in the presence of stable thermal stratification is of considerable importance in chemical and hydrometallurgical industries. Further, the importance of stratification in non-Darcy porous media is explored by several authors (*e.g.*, Takhar and Pop [15] and Rathish Kumar and Shalini [16]). For an exhaustive discussion of the convective transport on a vertical surface embedded in a doubly stratified porous medium, the reader is referred to the works of Lakshmi Narayana and Murthy [17] and Srinivasacharya and RamReddy [18] (also see the references cited therein). But very little attention has been paid to study the significance of the combined effects of MHD and thermal stratification on free convection in a nanofluid-saturated non-Darcy porous medium. Recently, the MHD convection flow and heat transfer of an incompressible viscous nanofluid past a semi-infinite vertical stretching sheet in the presence of thermal stratification are examined by Rosmila *et al.* [19]. These nanofluids appear to have a very high thermal conductivity and may be able to meet the rising demand as an efficient heat transfer agent. Scientists and engineers have started showing interest in the study of the heat transfer characteristics of these nanofluids. But a clear picture about the heat transfer through these nanofluids is yet to emerge.

Motivated by all these works, this article attempts to present the effect of the magnetic field on natural convection along a vertical plate in a non-Darcy porous medium, saturated with thermally stratified nanofluids. Some similar studies are found in the case of a porous medium without nanofluids, in the literature, but, to the best of the author's knowledge, this problem has not been considered before. This type of investigation is useful in understanding heat transfer characteristics around a hot radioactive subsurface storage site or around a cooling magmatic intrusion, where the theory of convection heat transport is involved. Hence, this boundary condition is physically realistic and has more practical relevance. The implicit, iterative finite-difference method discussed by Blottner [20] is employed to solve the non-linear system of this particular problem. The effects of magnetic, thermal stratification and non-Darcy parameters are examined and are displayed through graphs. The results are compared with relevant results in the existing literature and are found to be in good agreement.

2 Mathematical formulation

The coordinate system is chosen such that the x-axis is along the vertical plate and the y-axis normal to the plate. The physical model and the coordinate system are shown in fig. 1. Consider a two-dimensional steady laminar natural convective flow of an electrically conducting fluid, from the vertical flat plate in a non-Darcy porous medium, saturated with a stable thermally stratified nanofluid. The plate is maintained at uniform wall temperature T_w and nanoparticle concentration ϕ_w. The temperature of the ambient medium is assumed to be linearly stratified in the form $T_\infty(x) = T_{\infty,0} + Ax$, where A is constant and varied to alter the intensity of the stratification in the medium. The ambient values, attained as y tends to infinity, of T and ϕ are denoted by $T_{\infty,0}$, and ϕ_∞, respectively. Further, a uniform magnetic field is applied normal to the plate. The magnetic Reynolds number is assumed to be small, so that the induced magnetic field can be neglected. Finally, the fluid and the porous structure are everywhere in local thermodynamic equilibrium and the porous medium is assumed to be transparent. The fluid flow is moderate, so the pressure drop is proportional to the linear combination of fluid velocity and the square of the velocity (the Forchhiemer flow model is considered).

By employing laminar boundary layer flow assumptions, the Oberbeck-Boussinesq approximation, using the Darcy-Forchheimer and Dupuit-Forchheimer models [5], the governing equations for the nanofluid flow problem under

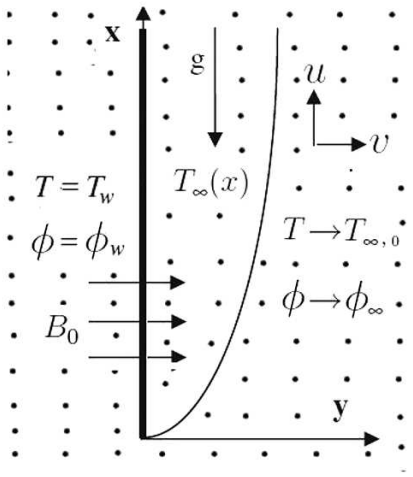

Fig. 1. Physical model and coordinate system.

investigation [3,6,7] are given by

$$\frac{\partial u}{\partial x} + \frac{\partial v}{\partial y} = 0, \tag{1}$$

$$\left(1 + \frac{\sigma\,\mu_e^2 B_0^2 K}{\mu}\right) u + \frac{c\sqrt{K}}{(\mu/\rho f_\infty)}\, u^2 = \frac{K(1-\phi_\infty)\,\rho f_\infty\, g\,\beta}{\mu}\,(T - T_\infty) - \frac{(\rho_P - \rho f_\infty)\,gK}{\mu}\,(\phi - \phi_\infty), \tag{2}$$

$$u\frac{\partial T}{\partial x} + v\frac{\partial T}{\partial y} = \alpha_m \frac{\partial^2 T}{\partial y^2} + J\left[D_B \frac{\partial \phi}{\partial y}\frac{\partial T}{\partial y} + \frac{D_T}{T_{\infty,0}}\left(\frac{\partial T}{\partial y}\right)^2\right], \tag{3}$$

$$\frac{1}{\varphi}\left(u\frac{\partial \phi}{\partial x} + v\frac{\partial \phi}{\partial y}\right) = D_B \frac{\partial^2 \phi}{\partial y^2} + \frac{D_T}{T_{\infty,0}}\frac{\partial^2 T}{\partial y^2}, \tag{4}$$

where u and v are the Darcy velocity components in the x- and y-direction, respectively, T is the temperature, ϕ is the nanoparticle concentration, g is the acceleration due to gravity, K is the permeability, c is the empirical constant associated with the Forchheimer porous inertia term, σ is the electrical conductivity of the fluid, μ_e is the magnetic permeability, B_0 is the strength of the magnetic field, φ is the porosity, $\alpha_m = k_m/(\rho c)_f$ is the thermal diffusivity of the fluid, $\nu = \mu/\rho f_\infty$ is the kinematic viscosity coefficient and $J = \varphi(\rho c)_p/(\rho c)_f$. Further, ρf_∞ is the density of the base fluid and ρ, μ, k_m and β are the density, viscosity, thermal conductivity and volumetric thermal expansion coefficient of the nanofluid, while ρ_p is the density of the nanoparticles, $(\rho c)_f$ is the heat capacity of the fluid and $(\rho c)_p$ is the effective heat capacity of the nanoparticle material. The coefficients that appear in eqs. (3) and (4) are the Brownian diffusion coefficient D_B and the thermophoretic diffusion coefficient D_T.

The associated boundary conditions are

$$v = 0, \qquad T = T_w, \qquad \phi = \phi_w \qquad \text{at} \qquad y = 0, \tag{5a}$$

$$u = 0, \qquad T = T_\infty(x), \qquad \phi = \phi_\infty \qquad \text{as} \qquad y \to \infty, \tag{5b}$$

where the subscripts w, $(\infty, 0)$ and ∞ indicate the conditions at the wall, at some reference point in the medium, and at the outer edge of the boundary layer, respectively.

Using the analysis of Nield and Bejan [5] and Nield and Kuznetsov [6], the following non-dimensional transformations can be introduced:

$$\begin{aligned}
\eta &= \frac{y}{x} Ra_x^{1/2}, \\
\psi(x,\eta) &= \alpha_m Ra_x^{1/2} f(x,\eta), \\
\theta(x,\eta) &= \frac{T - T_{\infty,0}}{T_w - T_{\infty,0}} - \frac{Ax}{T_w - T_{\infty,0}}, \\
S(x,\eta) &= \frac{\phi - \phi_\infty}{\phi_w - \phi_\infty},
\end{aligned} \tag{6}$$

where $Ra_x = \frac{(1-\phi_\infty)\rho f_\infty\, g\, K\, \beta(T_w - T_{\infty,0})\, x}{\mu \alpha_m}$ is the local Rayleigh number.

In view of the continuity eq. (1), we introduce the stream function ψ by

$$u = \frac{\partial \psi}{\partial y}, \qquad v = -\frac{\partial \psi}{\partial x}. \tag{7}$$

Substituting eq. (7) in eqs. (2)–(4) and then using the non-dimensional transformations (6), we get the following system of non-dimensional equations:

$$(1 + Ha) f' + Gr\, f'^2 = \theta - Nr \cdot S, \tag{8}$$

$$\theta'' + \frac{1}{2} f\, \theta' + Nb \cdot \theta' S' + Nt \cdot \theta'^2 = \varepsilon\, f' + \varepsilon \left(f' \frac{\partial \theta}{\partial \varepsilon} - \theta' \frac{\partial f}{\partial \varepsilon} \right), \tag{9}$$

$$S'' + \frac{1}{2} Le \cdot f\, S' + \frac{Nt}{Nb}\, \theta'' = Le\, \varepsilon \left(f' \frac{\partial S}{\partial \varepsilon} - S' \frac{\partial f}{\partial \varepsilon} \right), \tag{10}$$

where the primes indicate partial differentiation with respect to η alone. Further, $Gr = \frac{c\sqrt{K}}{\nu} \frac{\alpha_m}{x} Ra_x$ and $Ha = \frac{\sigma\, \mu_e^2\, B_0^2\, K}{\mu}$ are the non-Darcy and the magnetic parameter. In usual definitions, $Le = \frac{\alpha_m}{\varphi\, D_B}$, $Nr = \frac{(\rho_p - \rho f_\infty)(\phi_w - \phi_\infty)}{\rho f_\infty\, \beta(1-\phi_\infty)(T_w - T_{\infty,0})}$ are the Lewis number and the buoyancy parameter. Finally, $\varepsilon = \frac{Ax}{T_w - T_{\infty,0}}$, $Nb = \frac{J\, D_B (\phi_w - \phi_\infty)}{\alpha_m}$ and $Nt = \frac{J\, D_T}{\alpha_m T_{\infty,0}} (T_w - T_{\infty,0})$ are the thermal stratification, the Brownian motion and the thermophoresis parameters.

The boundary conditions (5) in terms of f, θ and S become

$$\eta = 0: \qquad f(\varepsilon, 0) = -2\varepsilon \frac{\partial f}{\partial \varepsilon}, \qquad \theta(\varepsilon, 0) = 1 - \varepsilon, \qquad S(\varepsilon, 0) = 1, \tag{11a}$$

$$\eta \to \infty: \qquad f'(\varepsilon, \infty) \to 0, \qquad \theta(\varepsilon, \infty) \to 0, \qquad S(\varepsilon, \infty) \to 0. \tag{11b}$$

The local heat and local nanoparticle mass fluxes from the vertical plate can be obtained from

$$q_w = -k_m \left(\frac{\partial T}{\partial y} \right)_{y=0}, \qquad q_m = -D_B \left(\frac{\partial \phi}{\partial y} \right)_{y=0}. \tag{12}$$

The dimensionless local Nusselt number, $Nu_x = \frac{q_w\, x}{k_m (T_w - T_{\infty,0})}$, and the local nanoparticle Sherwood number, $Sh_x = \frac{q_m\, x}{D_B (\phi_w - \phi_\infty)}$, are given by

$$\frac{Nu_x}{Ra_x^{1/2}} = -\theta'(\varepsilon, 0) \qquad \text{and} \qquad \frac{Sh_x}{Ra_x^{1/2}} = -S'(\varepsilon, 0). \tag{13}$$

3 Results and discussion

Equations (8)–(10) can be treated as an initial-value problem with ε playing the role of time. This general non-linear problem cannot be solved in closed form and, therefore, a numerical solution is necessary to describe the physics of the problem. The implicit, tri-diagonal finite-difference method similar to that discussed by Blottner [20] has proven to be adequate and sufficiently accurate for the solution to this kind of problems. Therefore, it is adopted in the present work. All first-order derivatives with respect to ε are replaced by a two-point backward-difference formula, when marching in the positive ε-direction. Then, all second-order differential equations in η are discretized using three-point central difference quotients. This discretization process produces a tri-diagonal set of algebraic equations at each line of constant ε, which is readily solved by the well-known Thomas algorithm (see Blottner [20]). During the solution, iteration is employed to deal with the non-linearity aspect of the governing differential equations. The problem is solved line by line starting with line $\varepsilon = 0$, where similarity equations are solved to obtain the initial profiles of velocity, temperature and nanoparticles volume fraction and marching forward in ε, until the desired line of constant ε is reached. Variable step sizes in the η-direction with $\Delta\eta_1 = 0.001$ and a growth factor $G = 1.035$ such that $\Delta\eta_n = G\Delta\eta_{n-1}$, and constant step sizes in the ε-direction with $\Delta\varepsilon = 0.01$ are employed. These step sizes are arrived at, after many numerical experimentations performed to assess grid independence. The convergence criterion employed in the present work is based on the difference between the current and the previous iterations. When this difference reached 10^{-5} for all points in the η-directions, the solution was assumed converged and the iteration process was terminated. The above step sizes and convergence criterion were found to give accurate grid-independent results as verified by the comparison mentioned below.

Table 1. Comparison of the dimensionless similarity functions, $\theta'(\eta)$ and $f'(\eta)$, for natural convection along a vertical flat plate in a non-Darcy porous medium with $Nb \to 0$, $Nt = Nr = 0$, $\varepsilon = 0$, $Ha = 0$ and $S(\eta) \to 0$ (Plumb and Huenefeld [21]).

	$f'(0)$		$\theta'(0)$	
Gr	Plumb and Huenefeld [21]	Present	Plumb and Huenefeld [21]	Present
0.00	1.00000	1.00000	0.44390	0.44374
0.01	0.99020	0.99019	0.44232	0.44216
0.10	0.91608	0.91608	0.42969	0.42950
1.00	0.61803	0.61803	0.36617	0.36575
10.00	0.27016	0.27016	0.25126	0.25065
100.00	0.09512	0.09512	0.15186	0.15145

With $Nb \to 0$, $Nt = Nr = 0$, $\varepsilon = 0$, $Ha = 0$ and $S(\eta) \to 0$ (*i.e.*, for the regular Newtonian fluid), eqs. (8)–(10), governing the present investigation of the thermally stratified nanofluid-saturated non-Darcy porous medium, reduce to those limiting case of natural convection flow by Plumb and Huenefeld [21], who investigated non-Darcy natural convection from vertical isothermal surfaces in saturated porous media, in the absence of stratification and MHD effects. Also, the results have been compared with those Plumb and Huenefeld [21], and it is found that they are in good agreement, as shown in table 1. Therefore, the developed code can be used with great confidence to study the problem considered in this paper.

We have computed the solutions for the dimensionless velocity, temperature and nanoparticle volume fraction functions and heat and nanoparticle mass transfer rates as shown graphically in figs. 2–10. The effects of the thermal stratification parameter ε, magnetic parameter Ha, non-Darcy parameter Gr, Brownian motion parameter Nb, thermophoresis parameter Nt and Lewis number Le and buoyancy ration Nr have been discussed.

The variation of the non-dimensional velocity, temperature and nanoparticle concentration for $Gr = 1$, $Nr = 0.1$, $Nt = 0.3$, $Le = 10$ and $\varepsilon = 0.5$, with magnetic parameter Ha and Brownian motion Nb, is illustrated in fig. 2. It can be observed from fig. 2(a) that the velocity of the fluid is reduced with enhancement in the value of the magnetic parameter. This happens because the application of a transverse magnetic field to an electrically conducting fluid results in a resistive-type force, which tends to slow down the motion of the fluid in the boundary layer and increases the temperature and concentration within the respective boundary layers. As explained above, the transverse magnetic field gives rise to a resistive force, known as the Lorentz force, of an electrically conducting fluid. This force makes the fluid experience a resistance by increasing the friction between its layers and, thus, increases its temperature and nanoparticle volume fraction. Furthermore, increasing the value of the Brownian motion Nb causes a thickening of momentum and thermal boundary layers, whereas thinning of the nanoparticle volume fraction boundary layer. Physically, it is true due to the fact that the large values of the Brownian motion parameter impacts a large extent of the fluid, it resulting in the thickening of the momentum and thermal boundary layers. Hence, for this particular flow configuration, the magnetic field reduces the fluid motion in the boundary layer. Furthermore, the present analysis shows that the flow field is appreciably influenced by the Brownian motion Nb. Therefore, the magnetic field is used to control boundary layer separation.

In figs. 3 and 4, the non-dimensional heat and nanoparticle mass transfer rates are plotted against the thermal stratification parameter ε, for different values of the magnetic parameter Ha and the Brownian motion Nb, with $Gr = 1$, $Nr = 0.1$, $Nt = 0.3$ and $Le = 10$. It may be noted that $\varepsilon = 0$ corresponds to the case of absence of stratification. Physically, positive values of the thermal stratification parameter have the tendency to increase the boundary layer thickness, due to the enhancement in the temperature difference between the plate and the free stream, in the presence of nanofluids. This causes a decrease in the Nusselt number as shown in fig. 3. These findings for the case of clear fluids in the absence of nanoparticles are opposite to the results obtained by the authors of refs. [16–18]. Therefore, the heat transfer rate is at a lower level, when this effect is considered ($\varepsilon \neq 0$), than that of when this effect is neglected ($\varepsilon = 0$). A similar trend can be seen in the case of the mass transfer rate. The results indicated that an increase in Ha increases the heat and nanoparticle mass transfer coefficients. It can be observed, from fig. 3, that the heat transfer rate decreases near the vertical plate and it increases far away from the plate with increasing Brownian motion Nb, showing a reverse behavior near the two boundaries, which results in diffusion penetrating deeper into the fluid and causing the thermal boundary layer to be thicker near the plate. In order to get physical insight into the problem, the convergence history plots for dimensionless velocity, temperature and nanoparticle volume fraction profiles for different flow parameters are provided in figs. 3 to 4. Further, the opposite trend is observed in the case of the nanoparticle mass transfer rate.

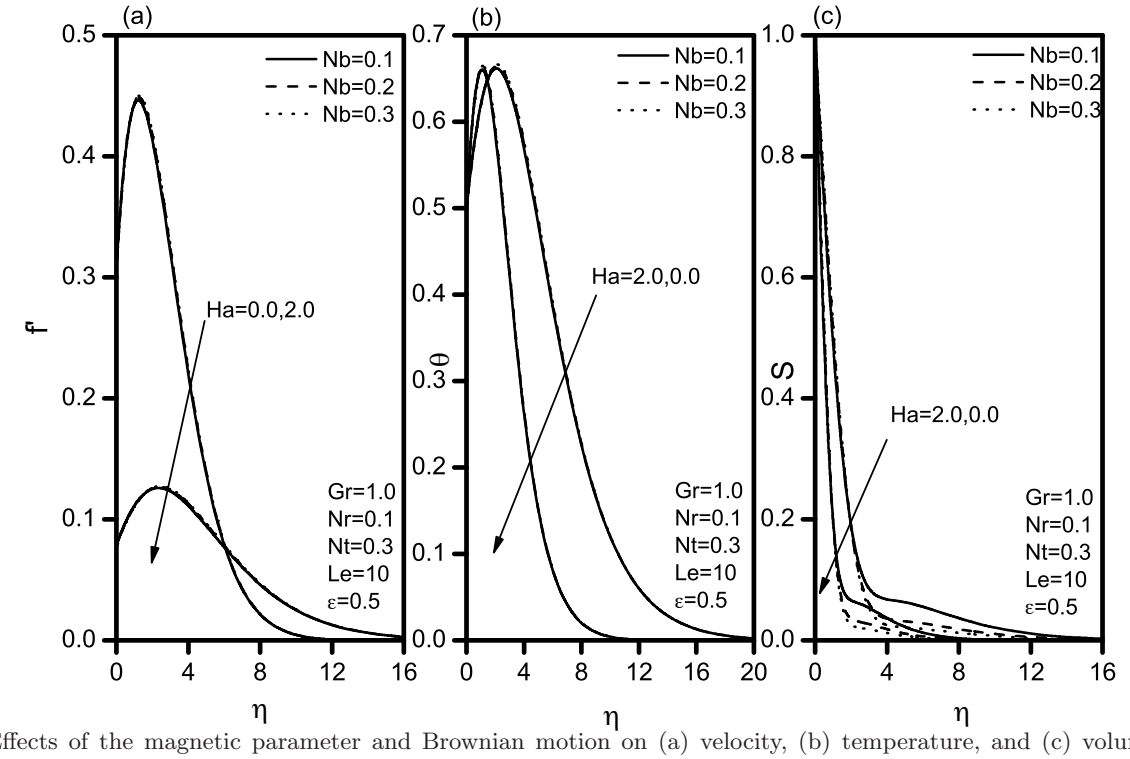

Fig. 2. Effects of the magnetic parameter and Brownian motion on (a) velocity, (b) temperature, and (c) volume fraction profiles.

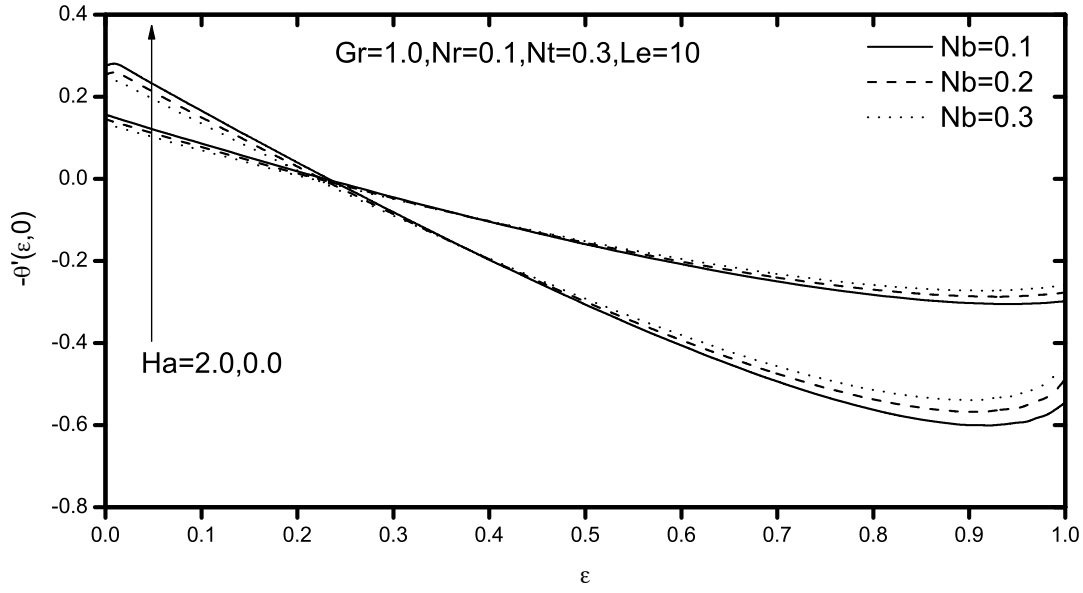

Fig. 3. Variation of the non-dimensional heat transfer coefficient, with ε for different values of magnetic parameter and Brownian motion.

Figure 5(a) exhibits the dimensionless velocity distribution for different values of the Forchheimer number Gr and Lewis number Le, with the fixed values of other parameters. An increase in the Forchheimer number increases the resistance to the flow and, hence, a decrease in the fluid velocity ensues, since Gr represents the inertial drag. Here $Gr = 0$ represents the case where the flow is Darcian. The velocity is maximum in this case, due to the total absence of inertial drag. The dimensionless temperature for different values of the Forchheimer number, Gr, for the fixed values of other parameters is displayed in fig. 5(b). An increase in the Forchheimer number, Gr, increases temperature values, since as the fluid is decelerated the energy is dissipated as the heat and it serves to increase temperatures. As such, the temperature is minimized for the lowest value of Gr and maximized for the highest value of Gr, as shown in fig. 5(b). Figure 5(c) depicts the dimensionless volume fraction for different values of the Forchheimer number Gr for

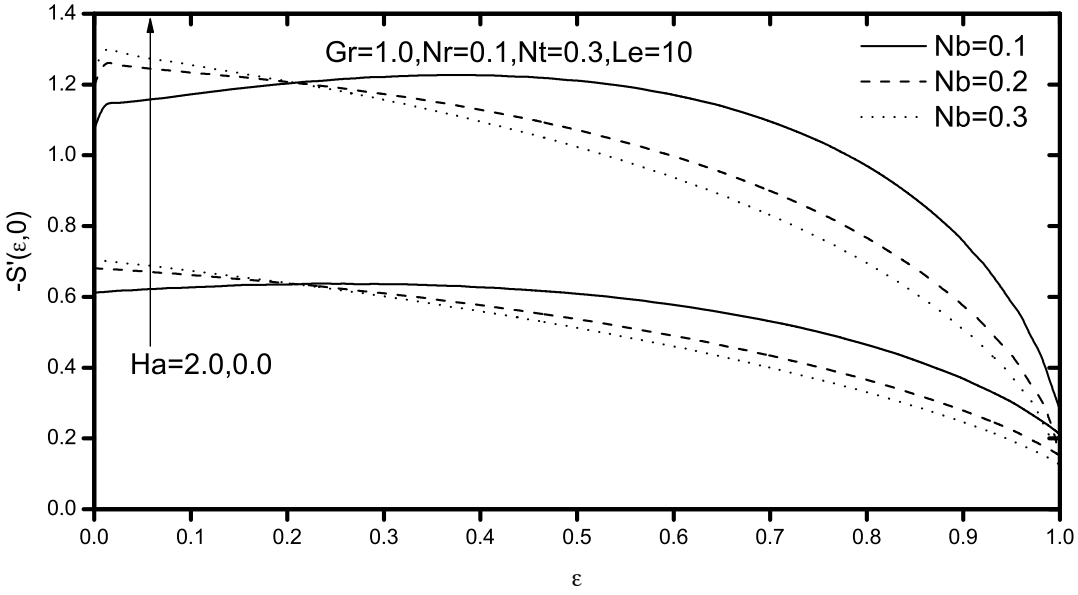

Fig. 4. Variation of the non-dimensional nanoparticle mass coefficient, with ε for different values of magnetic parameter and Brownian motion.

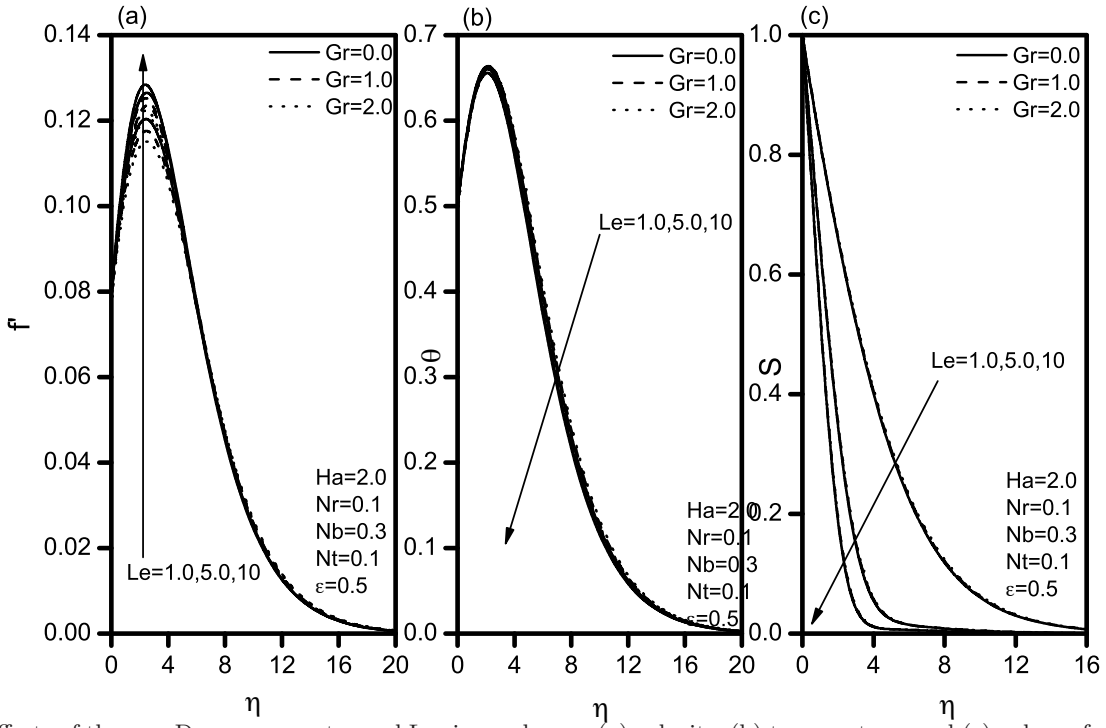

Fig. 5. Effects of the non-Darcy parameter and Lewis number on (a) velocity, (b) temperature, and (c) volume fraction profiles.

fixed values of other parameters. As the parameters Gr increases, the volume fraction profile increases for the specified conditions. An increase in the non-Darcy parameter reduces the intensity of the flow, but it enhances the thermal and nanoparticle volume fraction boundary layer thicknesses. Hence the non-Darcy parameter has an important role in controlling the flow field. It is noticed, from fig. 5, that an increase in the Lewis number Le results in an increase in the velocity, but in a decrease in the temperature and volume fraction within the boundary layer. The present analysis shows that the flow field is appreciably influenced by the Lewis number Le.

In fig. 6, the non-dimensional heat transfer coefficient is plotted against the thermal stratification parameter ε, for different values of the Forchheimer number Gr and Lewis number Le. It is shown that the heat transfer rate non-linearly decreases with the stratification parameter. Also, the results indicate that an increase in Gr increases the

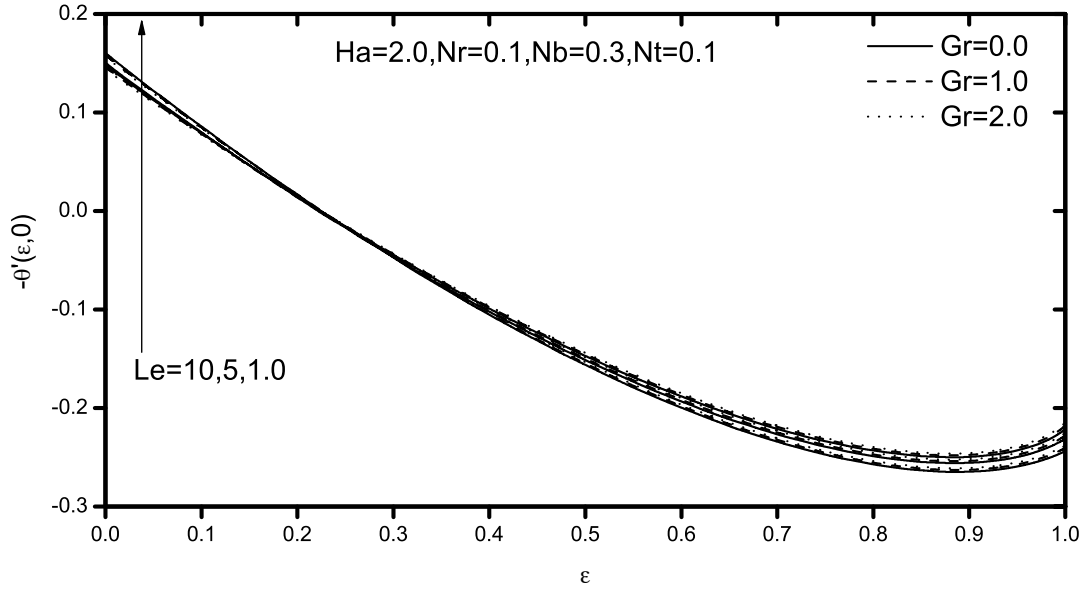

Fig. 6. Variation of the non-dimensional heat transfer coefficient, with ε for different values of non-Darcy parameter and Lewis number.

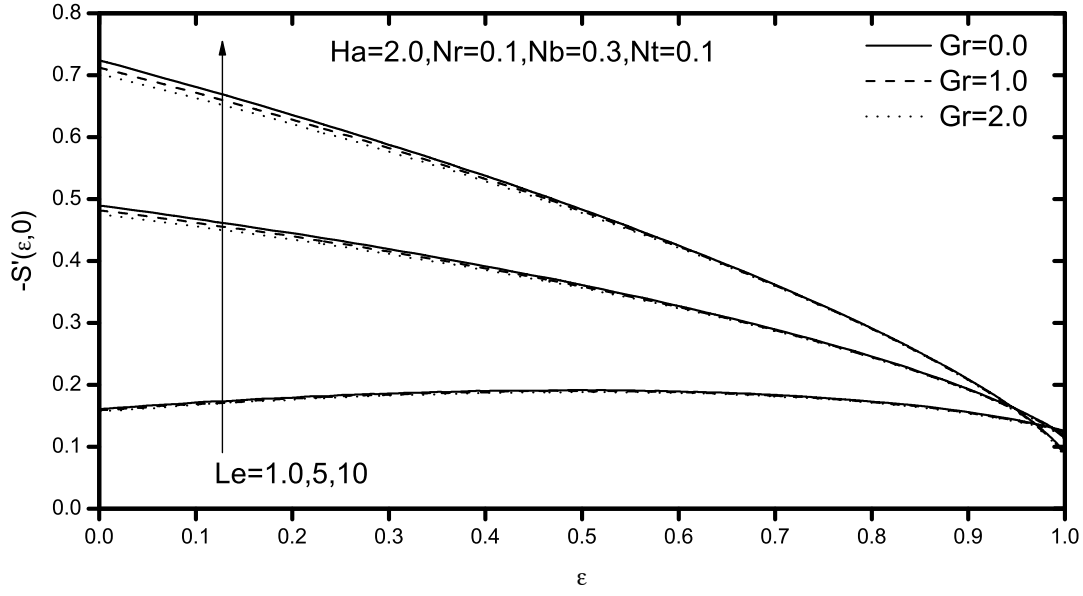

Fig. 7. Variation of the non-dimensional nanoparticle mass transfer coefficient, with ε for different values of non-Darcy parameter and Lewis number.

heat transfer coefficient but, with increasing values of Le, the non-dimensional mass transfer coefficient decreases. It is clear, from fig. 7, that for increasing values of Gr the non-dimensional mass transfer coefficient decreases, whereas, with increasing values of Le, the non-dimensional mass transfer coefficient increases. Finally, the non-dimensional mass transfer coefficient decreases non-linearly with increasing values of ε. Hence the non-Darcy parameter has an important role in controlling the flow field.

Figure 8 presents the effect of the buoyancy ratio Nr and thermophoresis Nt on the velocity, temperature and volume fraction distributions. It is observed that the momentum boundary layer thickness increases with an increase of Nt and Nt. As the parameter Nt increases, the thermal and nanoparticle volume fraction boundary layer thickness increase for the specified conditions. We notice that positive Nt indicates a cold surface, while negative to a hot surface. For hot surfaces, thermophoresis tends to blow the nanoparticle volume fraction boundary layer away from the surface, since a hot surface repels the submicron-sized particles from it, thereby forming a relatively particle-free layer near the

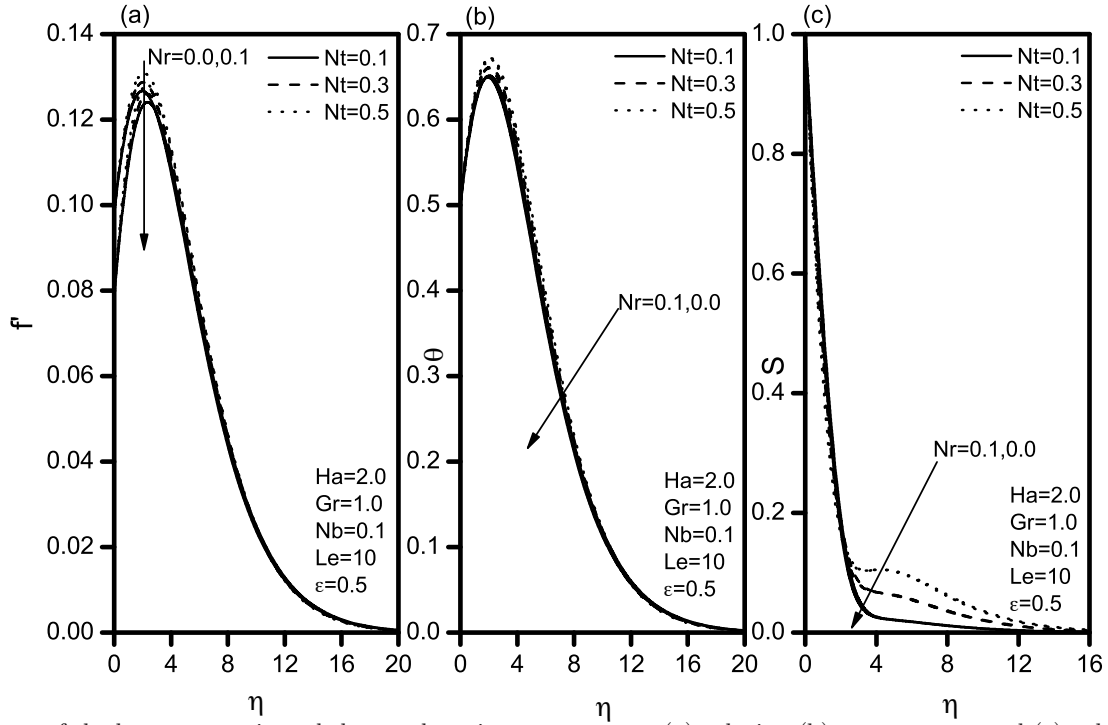

Fig. 8. Effects of the buoyancy ratio and thermophoresis parameters on (a) velocity, (b) temperature, and (c) volume fraction profiles.

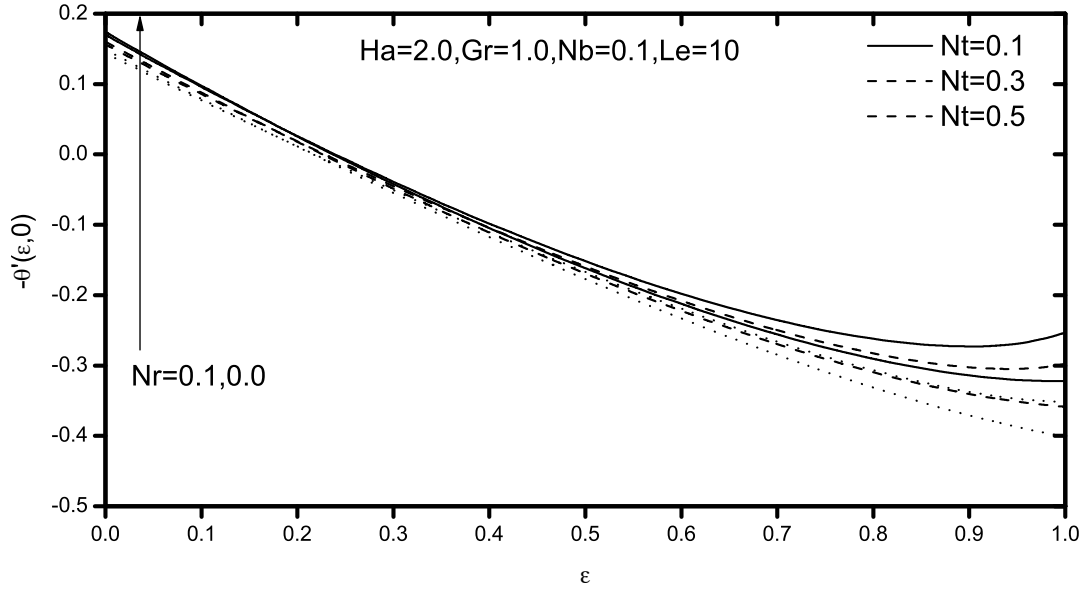

Fig. 9. Variation of the non-dimensional heat transfer coefficient, with ε for different values of buoyancy ratio and thermophoresis parameters and fixed values of other parameters.

surface. As the nanoparticle buoyancy ratio Nr increases, it can be observed from fig. 8 that the maximum of velocity decreases in amplitude. The location of the maximum velocity moves further away from the wall. It is clearly seen, from fig. 8, that an increase in Nr tends to an increase in the thermal and nanoparticle volume fraction boundary layer thickness.

The non-dimensional heat transfer coefficient is plotted against the thermal stratification parameter ε in fig. 9, for different values of the buoyancy ratio Nr and thermophoresis Nt. It can be observed from this figure that the heat transfer rate decreases with increasing values of Nt and Nr. In fig. 10, the non-dimensional mass transfer coefficient is plotted against the thermal stratification parameter ε, for different buoyancy ratio Nr and thermophoresis Nt. It is

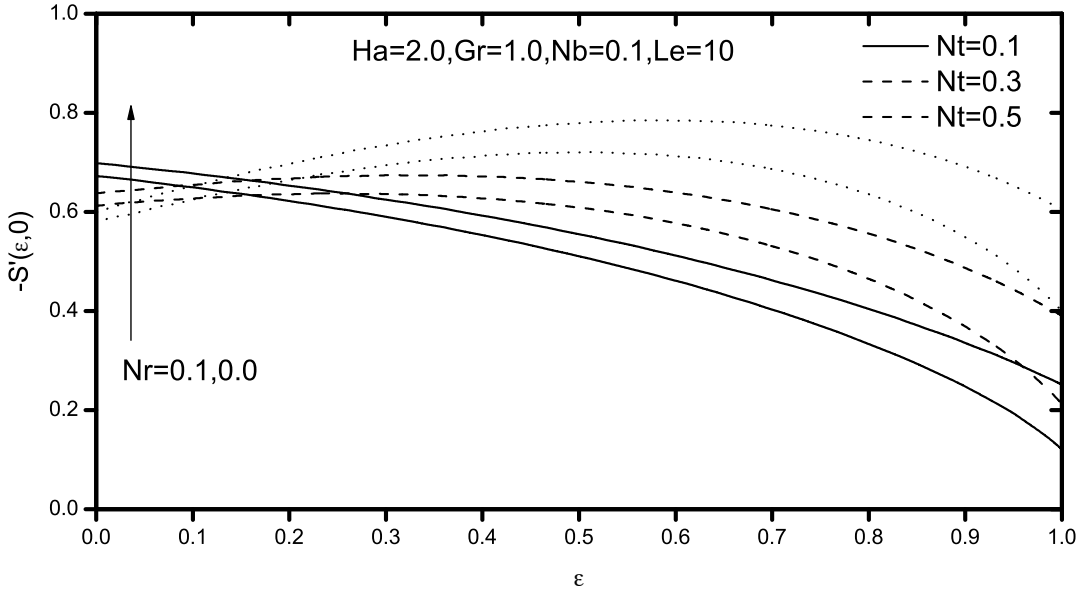

Fig. 10. Variation of the non-dimensional nanoparticle mass transfer coefficient, with ε for different values of buoyancy ratio and thermophoresis parameters and fixed values of other parameters.

evident from this figure that for increasing values of Nr the non-dimensional mass transfer coefficient decreases. Also, one can see that the nanoparticle mass transfer coefficient increases with an increase in Nt. Finally, the non-dimensional heat and nanoparticle mass transfer coefficient decreases non-linearly with increasing values of ε.

4 Conclusions

In this paper, we discussed the effect of the magnetic field on natural convection in a thermally stratified nanofluid-saturated non-Darcy porous medium. Using the dimensionless variables, the governing equations are transformed into a set of non-linear parabolic equations, where the numerical solution has been presented using the implicit, iterative finite-difference method discussed by Blottner [20], for a wide range of parameters. The features of flow characteristics are analyzed by plotting graphs and discussed in detail. The main findings are summarized as follows:

- Increasing the magnetic field strength leads to a decrease in the velocity distribution and the rates of heat and mass transfer, but to an increase in the temperature and nanoparticle volume fraction distributions from the vertical plate. Similar effects can be found in the case of the nanoparticle buoyancy parameter Nr.
- Increasing the non-Darcy parameter Gr leads to decrease the velocity distribution and nanoparticle mass transfer rate, but to increase the temperature, nanoparticle volume fraction distributions and heat transfer rate. An opposite nature can be found in the case of the Lewis number Le as compared to Gr.
- The heat and nanoparticle mass transfer rates increase by increasing the thermal stratification parameter ε.
- An increase in the Brownian motion parameter Nb, enhances the velocity and temperature distributions and the heat transfer rate, but it reduces nanoparticle volume friction and nanoparticle mass transfer rate in boundary layer.
- The velocity, temperature and volume fraction distributions and nanoparticle mass transfer rate increases, but the non-dimensional heat transfer rate decreases in the boundary layer by increasing the thermophoresis parameter Nt.
- Physical significance and application of MHD, thermal stratification in a nanofluid-saturated non-Darcy porous medium, with respect to boundary layer flow problems can be found in several engineering and industrial processes as mentioned in the introduction. Moreover, many patents have been devoted to the methods of preparation of new nanofluids heat transfers. Nanofluids are now being developed for medical applications, including cancer therapy and safer surgery by cooling.

References

1. S.U.S. Choi, *Enhancing thermal conductivity of fluid with nanoparticles*, in *Developments and Applications of Non-Newtonian Flows, FED-V. 231/MD-V. 66*, edited by D.A. Siginer, H.P. Wang (1995) pp. 99–105.
2. S.K. Das, S.U.S. Choi, W. Yu, T. Pradeep, *Nanofluids: Science and Technology* (Wiley, New Jersey, 2007).
3. J. Buongiorno, J. Heat Transfer **128**, 240 (2006).
4. S. Kakac, A. Pramuanjaroenkij, Int. J. Heat Mass Transfer **52**, 3187 (2009).
5. D.A. Nield, A. Bejan, *Convection in Porous Media* (Springer-Verlag, New York, 2013).
6. D.A. Nield, A.V. Kuznetsov, Int. J. Heat Mass Transfer **52**, 5792 (2009).
7. D.A. Nield, A.V. Kuznetsov, Int. J. Heat Mass Transfer **52**, 5796 (2009).
8. A.J. Chamkha, R.S.R. Gorla, K. Ghodeswar, Transp. Porous Media **86**, 13 (2011).
9. W.A. Khan, A. Aziz, Int. J. Therm. Sci. **50**, 2154 (2011).
10. R.S.R. Gorla, A.J. Chamkha, J. Mod. Phys. **2**, 62 (2011).
11. A.J. Chamkha, A.M. Aly, Chem. Eng. Commun. **198**, 425 (2010).
12. M.A.A. Hamada, I. Pop, A.I. Md-Ismail, Nonlinear Anal. Real World Appl. **12**, 1338 (2011).
13. M.J. Uddin, W.A. Khan, A.I. Ismail, PLoS ONE **7**, e49499 (2012).
14. P.K. Kameswaran, M. Narayana, P. Sibanda, P.V.S.N. Murthy, Int. J. Heat Mass Transfer **55**, 7587 (2012).
15. H.S. Takhar, I. Pop, Mech. Res. Commun. **14**, 81 (1987).
16. B.V. Rathish Kumar, Shalini, Appl. Math. Comput. **171**, 180 (2004).
17. P.A. Lakshmi Narayana, P.V.S.N. Murthy, J. Heat Transfer **128**, 1204 (2006).
18. D. Srinivasacharya, Ch. RamReddy, Int. Commun. Heat Mass Transfer **37**, 873 (2010).
19. A.B. Rosmila, R. Kandasamy, I. Muhaimin, Appl. Math. Mech. Engl. Ed. **33**, 593 (2012).
20. F.G. Blottner, AIAA J. **8**, 193 (1970).
21. O.A. Plumb, J.C. Huenefeld, Int. J. Heat Mass Transfer **24**, 765 (1981).